Top Catal (2008) 50:90–97
DOI 10.1007/s11244-008-9109-9

ORIGINAL PAPER

Steric Effect on the Catalytic Performance of the Selective Oxidation of Alcohols Over Novel Crystalline Mo–V–O Oxide

Feng Wang · Wataru Ueda

Published online: 13 June 2008

Abstract The Mo–V–O crystalline oxide with novel pore structure and consisting uniform six- and seven-member rings on the *a–b* plane is investigated for the selective oxidation of alcohols of different steric hindrance in liquid phase. The research target is to correlate catalytic activity with the pore structure of the crystal. Specially, substituted pyridines are employed as probe molecules to study poison effect which is closely related to the steric hindrance. As a result, the oxidation of benzyl alcohol, 1-hexanol and cyclohexanol produces aldehydes or ketones as main products. The oxidation of substrates with methyl groups on the carbon next to alcohol group mainly affords dehydrated products as olefins. The catalytic results with adding substituted pyridines in the oxidation of benzyl alcohol, 1-hexanol and 2-hexanol suggest that the active sites are located around the pore area, and are reachable by pyridine, not by substituted pyridines, such as 2-methylpyridine, 2-ethylpyridine and 2, 6-dimethylpyridine. Competitive adsorption on active sites between pyridine and benzyl alcohol remarkably decreases catalytic activity, which 2, 6-dimethylpyridine affects slightly. We have discussed that the adsorption-activation model of substrate is greatly dependent on its steric hindrance.

Keywords Mo–V–O catalyst · Selective oxidation · Benzyl alcohol · 1-Hexanol · 2-Hexanol · Steric effect · Novel pore structure

F. Wang (✉)
CREST, Japan Science and Technology Corporation (CREST-JST), Kawaguchi, Saitama 332-0012, Japan
e-mail: wangfeng@cat.hokudai.ac.jp

F. Wang · W. Ueda (✉)
Catalysis Research Center, Hokkaido University, N-21, W-10, Sapporo 001-002, Japan
e-mail: ueda@cat.hokudai.ac.jp

1 Introduction

Currently, the Mo–V–O oxide based catalysts have invoked many interests in the selective oxidation of hydrocarbons [1–6]. One of the promising applications is to replace propene feedstock with propane for producing acrylic acid and acrylonitrile [7–10]. In these researches, the selectivity remains central interest. To achieve high selectivity for the desired product, it is important to understand the intricacy of catalytically active sites and their environment [11]. Grasselli et al. have reported that the Mo–V–Nb–Te catalyst is comprised of at least two phases (*M1* and *M2*) and that *M1* is the paraffin-activating phase while *M2* is the olefin conversion phase [12–26]. Our research group has developed a method of preparing pure orthorhombic phase of Mo–V–O oxides under hydrothermal conditions [27–35]. Although the complete understanding of the crystalline structure of Mo–V–O oxides has not been realized yet, it is classified that the unique pore and its neighbor area is necessary for the prominent catalytic performance.

Recently, we have reported the selective oxidation of ethane to acetic acid and propane to acrylic acid by the doped Mo–V–O oxide catalysts (doped metal: Al, Cr, Fe, Te, Sb, and Nb) [28–35], and have discussed that the a layer-type material constructed mainly with six- or seven-member rings is responsible for the high selectivity for the desired products. However, the catalytic applications using the Mo–V–O crystal were mainly focused on the selective oxidation of small molecules (carbon number is <5) at elevated temperature higher than 200 °C. On the other hand, the selective oxidation of large molecules under mild conditions, such as the oxidation of benzyl alcohol to benzaldehyde in liquid phase, has never been explored. These researches are extremely significant of broadening the knowledge of the Mo–V–O crystal, and further

correlating a relationship between catalytic activity and catalyst structure. In contrast to the known methods of alcohol oxidation over precious metal-based catalysts and organo-catalysts [36–41], which have achieved both excellent conversion and selectivity, the present research is devoted to understand the oxidation of alcohols over transition metal-based microporous catalysts.

The adsorption of substrate is a key step in catalysis. We postulate that if the active sites of the Mo–V–O oxide are located around 6- and 7-member rings, the possibility of substrates adsorption on these sites may decrease with increasing steric hindrance, and therefore catalytic results will be altered accordingly. Pyridine and its derivatives are adopted as poisons for acid sites to study the effect of acidity on catalytic performance [42]. Likewise, if pyridine and substituted pyridines are employed for these purposes, the poison consequences may be greatly dependent on their steric hindrance. In this research, we choose several model reactions, such as the oxidation of benzyl alcohol over crystalline and non-crystalline oxide, the oxidation of 1-hexanol and 2-hexanol, the oxidation of cyclohexanol and substituted cyclohexanols, and the addition of pyridine and substituted pyridines, to study the function of the pore in the oxidation reaction.

2 Experimental

2.1 Catalyst Preparation

All reagents were analytical grade, purchased from Wako Pure Chemical Industries, Ltd., and used without further purification. Distilled water was prepared using Yamato Autostill WG25 (Tokyo, Japan).

Catalyst preparation procedure: $VOSO_4{\cdot}nH_2O$ (64.83 wt.%) solution (V concentration 0.10 mol L^{-1}, 120 mL) was added to $(NH_4)_6Mo_7O_{24}{\cdot}4H_2O$ ammonium heptamolybdate tetrahydrate (AHM) solution (Mo concentration 0.42 mol L^{-1}, 120 mL). The above mixture was stirred for 10 min under ambient condition before being transferred to a 300-mL Teflon-lined autoclave. The mixture was bubbled with a flow of nitrogen (50 mL min^{-1}) for 10 min to remove oxygen. The autoclave was immediately sealed and placed in a 175 °C oven for 48 h. The black material formed on the Teflon liner was filtered out, and dried at 80 °C for 24 h. The purification of the dried sample was carried out by adding 1.0 g of the dry sample into an oxalic acid solution (0.4 mol L^{-1}, 50 mL). The solution was magnetically stirred at 60 °C for 30 min, filtered out and washed with 500 mL water. The filtrate was dried at 80 °C for 24 h, and then degassed at 400 °C (heating ramp rate 10 °C min^{-1}) in nitrogen (50 mL min^{-1}) for 2 h. The calcined sample was taken out after the oven temperature decreased below 150 °C. The sample was designated as MoVO–CR (crystalline).

A non-crystalline sample designated as MoVO–AM (amorphous) were prepared using the same precursors solution with that of the MoVO–CR, but crystallizing at ambient conditions (ca. 23 °C) for 48 h. The dark purple filtrate formed at the bottom of the Teflon liner was filtered out through filter paper, dried at 80 °C for 14 h, milled for 10 min, and calcined using the same procedure with that of the MoVO–CR.

2.2 Catalyst Characterization

Powder XRD patterns were recorded on a diffractometer (Rigaku, RINT Ultima+) with Cu$K\alpha$ radiation ($K\alpha$ 1.54056 Å). Field emission scanning electron microscopy (FE–SEM) was performed on a JSM-7400F (JEOL). Specific surface areas were measured by N_2 adorptioin at 77 K using BET method over Autosorb 6AG (Quantachrome Instruments). ^{1}H NMR sprectra were recorded using JEOL ECX-600 or JEOL ECX-400 at CRIS center of Hokkaido University. Reactant and product concentratons were measured by gas chromatography using flame ionization detector (Shimazu Classic–5000, 60 m TC WAX column), operated with a heating program: 100 °C for 10 min, ramp 10 °C min^{-1} to 230 °C (kept for 25 min).

2.3 Catalytic Test

Batch reactors were used for catalytic test (Fig. 1). The sidearm reactors could realize identical reaction condition for a number of tests up to eight. The reactor volume was ca. 15 mL. The gas balloon containing oxygen had a volume of ca. 1 L. It was calculated that <2% of total oxygen could be consumed based on 100% conversion of used alcohols. In a typical reaction, the catalyst and magnetic stir bar were initially loaded into the reactor. The oxygen provided by an oxygen tank was inflated into the reactor at room temperature through a needle connected with a sidemouth sealed with Teflon septum, through which a reactant

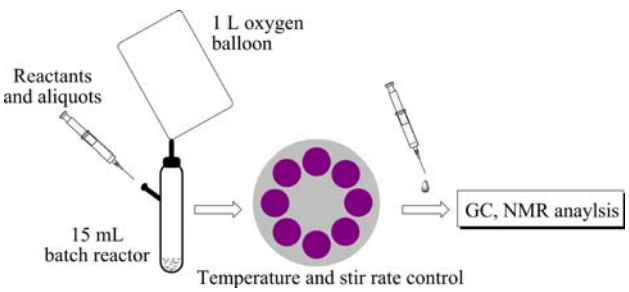

Fig. 1 Batch reactor experimental setup

mixture of alcohol, toluene, and *p*-xylene (internal standard) was injected by a syringe. All reactors were placed into an oil bath which was thermally controlled with constant temperature during reaction. Aliquots were collected at intervals. After reaction, the oil bath was removed away and the reaction mixture was cooled down before open for sampling. Catalyst was filtered out using 0.2 μm membrane filter; the filtrate was analyzed using gas chromatography mass spectrometry (GC–MS). ^{1}H NMR was employed to analyze acid products. ^{1}H NMR analysis of crude mixture after reaction was the following. Ca. 0.3 mL aliquot of reaction mixture was put into a small vial, and evaporated under 65 °C in a rotation evaporator in vacco. One microliter d^6-DMSO solvent was added to dissolve the remaining before spinning (21–24 °C).

3 Results and Discussion

3.1 The Catalyst Structure

Our previous studies [35] have shown that the MoVO–CR oxide belongs to an orthorhombic group of *Pbam* (*55*) with lattice constants: $a = 21.19$ Å, $b = 26.57$ Å and $c = 4.00$ Å (Fig. 2). Under hydrothermal conditions, the anisotropic growth along the *c*-axis direction forms rod-shaped crystal with 2–10 μm length, and 0.5–1 μm width along the *a*- and *b*-axis direction (Fig. 3). The rod is composed of ca. 4 Å slabs. Projected on the *a*–*b* plane, the crystal consists of the 6- or 7-member rings (6MRs and 7MRs); five MoO_6 octahedrons surround one MoO_7 pentagonal bi-pyramid by edge-sharing; the 6MRs and 7MRs are interconnected with MoO_6 and/or VO_6 octahedrons by corner-sharing. In contrast, the MoVO–AM resembles amorphous morphology (Fig. 4). The MoVO–AM catalyst has a BET specific surface area of 0.9 $m^2\ g^{-1}$, while the specific surface area of the MoVO–CR is 14.7 $m^2\ g^{-1}$. The hydrothermal treatment is necessary for constructing uniform pore structure. The diffraction patterns of the two catalysts are shown in Fig. 5. The MoVO–CR displays the typical patterns of an orthorhombic phase, while the MoVO–AM is amorphous phase.

3.2 The Catalytic Results of the Selective Oxidation of Benzyl Alcohol Over the MoVO–CR and the MoVO–AM

We recently reported that the high selectivities in the oxidation of substituted benzyl alcohols to benzaldehydes were achieved over the MoVO–CR [43]. The catalytic results manifested that the high selectivity for benzaldehyde was due to the pore structure of the Mo–V–O crystal. As shown in Table 1, the MoVO–CR exhibited high selectivity to benzaldehyde. However, the MoVO–AM gave 68% selectivity for benzaldehyde at the conversion of 20% in 18 h reaction. In a 24 h reaction, 32% conversion of benzyl alcohol was achieved with the 42% selectivity of benzaldehyde. The main products by the MoVO–AM catalyst were benzoic acid, benzyl benzoate and benzylated toluene [44, 45], suggesting the over-oxidation of benzaldehyde and the alkylation occurred.

3.3 The Selective Oxidation of 1-Hexanol and 2-Hexanol

To compare catalytic results of the oxidation of primary alcohol and secondary alcohol [41], the oxidation of 1-hexanol and 2-hexanol were employed as model reactions. The catalytic tests were conducted under three reaction conditions: (i) the reaction atmosphere was oxygen and the catalyst was the MoVO–CR; (ii) the reaction atmosphere was argon and the catalyst was the MoVO–CR; and (iii) the reaction atmosphere was oxygen and the catalyst was the MoVO–AM.

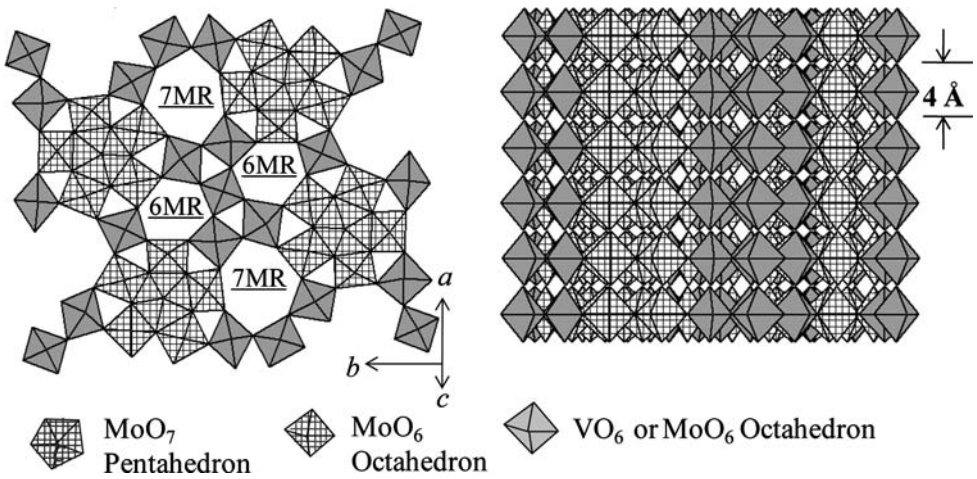

Fig. 2 The crystal structure of the orthorhombic phase molybdenum and vanadium oxide (MoVO–CR): (*left*) in view of crystal from the *c*-axis direction. 6- and 7-member rings (*6MR* and *7MR*) are labeled; (*right*) in view of crystal from the *a*-axis direction

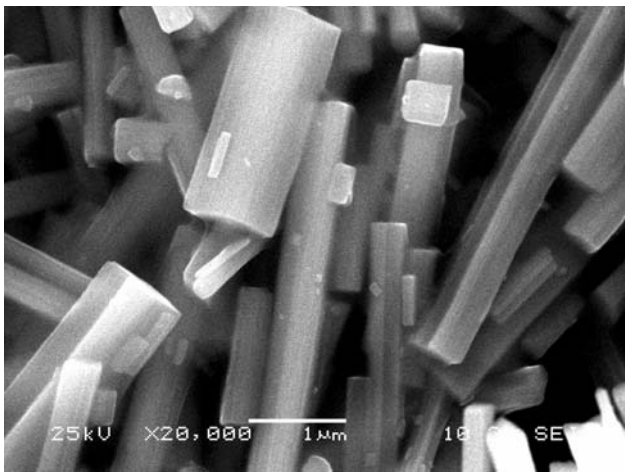

Fig. 3 FE–SEM image of the MoVO–CR

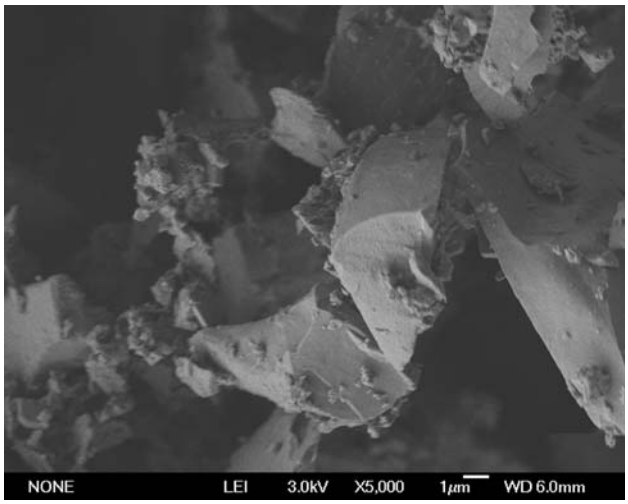

Fig. 4 FE–SEM image of the MoVO–AM

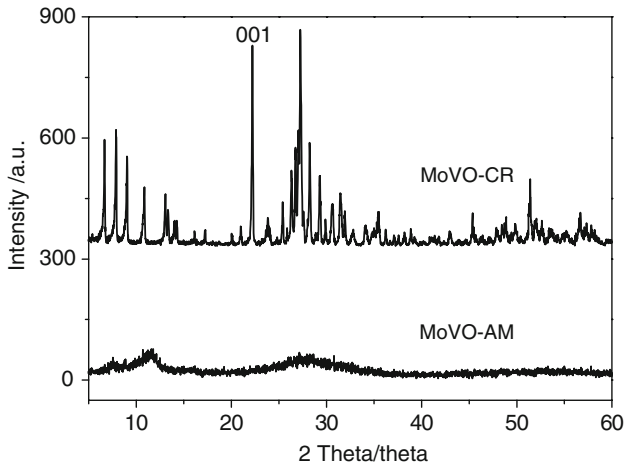

Fig. 5 XRD patterns of the MoVO–CR and the MoVO–AM

Table 1 Catalytic performance of the aerobic oxidation of benzyl alcohol over MoVO–CR and MoVO–AM

Catalyst	*t* (h)	Conv. (%)	Product distribution (%)				
			Bal	BA	BB	AT	Others
MoVO–CR	18	16	>99	0	0	0	0
MoVO–CR	24	22	>99	0	0	0	0
MoVO–AM	18	20	68	14	8	9	1
MoVO–AM	24	32	42	5	10	40	3

Reaction conditions: alcohol 0.7 mmol, toluene 1.6 mL, catalyst 0.03 g, 80 °C, O_2 pressure (1 atm). GC conversion and selectivity were measured with *p*-xylene (40 μL) as internal standard. Acid products were analyzed by ^{1}H NMR. Bal: benzaldehyde; BA: benzoic acid; BB: benzyl benzoate; AT: alkylated toluene

Catalytic results were listed in Table 2. The conversion of 1-hexanol and 2-hexanol in the reaction (i) were 11 and 22%, respectively. Nevertheless, the product distributions were quite different. 1-Hexanol gave 1-hexanal (aldehyde) as major product (selectivity 95%) with the remaining 5% for olefins and ether products; 2-hexanol offered 76% selectivity for olefins with 22% for 2-hexanone. The olefin ratio of 2-hexene over 1-hexene was ca. 4.4, resembling the Saytzeff elimination reaction character. If calculating the formation rate of aldehyde or ketone, the rate of 1-hexanol was ca. 2.5 times of that of 2-hexanol, illustrating the difference of steric hindrance between 1-hexanol and 2-hexanol on the *a–b* plane. The higher conversion of 2-hexanol than 1-hexanol suggested that the formation of a carbocation was probably involved since the secondary carbocation was much stable than the primary one. If the two reactions were conducted in argon in reaction (ii), the conversion of 1-hexanol was ca. 1%, and the product was 1-hexene. However, the 11% conversion of 2-hexanol was obtained with 97% selectivity for olefins, in which the ratio of 2-hexene over 1-hexene was ca. 4.6, which was approximate to the olefin ratio in reaction (i). We postulated that due to the steric effect, 1-hexanol was favorably adsorbed on the pore area in a perpendicular model, and 2-hexanol was inclined to be adsorbed onto non-pore area in a parallel model. The pore area contains unsaturated metal cation sites and oxygen anion sites. Such sites locating in approximate distance and space geometry are responsible for the activating of primary alcohols. By contrast, the reactions catalyzed by the MoVO–AM in reaction (iii) gave 39 and 31% conversion of 2-hexanol and 1-hexanol, respectively. The major products of both reactions were olefins, and the by-products distributing among ketone, aldehyde, and ether were much more complex than both reaction (i) and (ii), indicating the catalysis by the MoVO–AM was less selective and more complex.

Table 2 The oxidation of 1-hexanol and 2-hexanol over crystalline and non-crystalline catalyst in oxygen or argon atmosphere

	Substrate	Catalyst	Gas	Conv (%)	Product distribution (%)				
					Aldehyde	Ketone	1-ene	2-ene	Others
i	1-Hexanol	MoVO–CR	O_2	11	95	0	<5	0	<1
	2-Hexanol	MoVO–CR	O_2	22	0	22	14	62	2
ii	1-Hexanol	MoVO–CR	Ar	1	0	0	100	0	0
	2-Hexanol	MoVO–CR	Ar	11	0	4	17	79	0
iii	1-Hexanol	MoVO–AM	O_2	31	5	1	83	0	11
	2-Hexanol	MoVO–AM	O_2	39	0	3	19	78	<1

Reaction conditions: alcohol 0.7 mmol, toluene 1.6 mL, catalyst 0.03 g, 80 °C, 24 h, pressure (1 atm). GC conversion and selectivity were measured with *p*-xylene (40 μL) as internal standard. 1-ene: 1-hexene; 2-ene: 2-hexene

3.4 The Selective Oxidation of Substituted Cyclohexanols

The conversion and product selectivity had great difference among substituted cyclohexanols as listed in Table 3. The conversion increased from cyclohexanol (11%), 2-methylcyclohexanol (12%) to 2, 6-dimethylcyclohexanol (43%), in accordance with the increasing order of molecule steric hindrance. On the other hand, the selectivity of cyclohexanones decreased from 94 to 5%. These results were explained by the substrate adsorption–activation on the *a–b* plane of the MoVO–CR. The methyl groups hindered the C–OH to adsorb on the pore, and thus the substrate was adsorbed on the non-pore area where it was activated in parallel to surface so that the breakage of α carbon–hydrogen bond was geometrically suitable, leading to

Table 3 Selective oxidation of cyclohexanol and methyl-substituted cyclohexanol

Alcohol	Conv (%)	Sel (%)		GC yield (%)	
		Cyclohexanones	Cyclohexenes	Cyclohexanones	Cyclohexenes
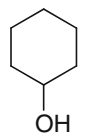	11	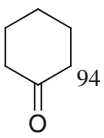		10	1
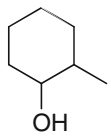	12	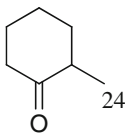	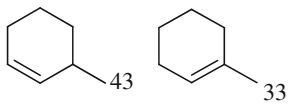	3	9
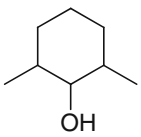	43	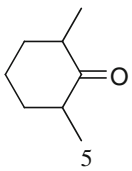	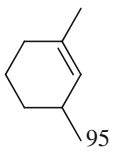	2	41

Reaction conditions: alcohol 0.7 mmol, catalyst 0.03 g, toluene 1.6 mL, 80 °C, 24 h, oxygen balloon (1 atm). Selectivity and conversion were determined by GC

olefins. It was noted that the product ratio of 1-methylcyclohexene to 3-methylcyclohexene in the oxidation of 2-methylcyclohexanol was ca. 4:3, which was contrary to the literatures of homogeneous reaction [46, 47], where the ratio was close to 3:1. Such difference was probably due to the steric effect, which played a key role in the heterogeneous solid surface reaction.

3.5 The Effect of Pyridine and its Derivatives as Additives in the Selective Oxidation of Benzyl Alcohol

In this research, we aimed at studying catalytic consequences of different substituted pyridines as probe molecules in the oxidation of benzyl alcohol. The four molecules were pyridine, 2-methylpyridine, 2-ethylpyridine, and 2, 6-dimethylpyridine, which did not have big difference in pK_a value (in water: 5.2, 5.9, 5.9, and 6.7, respectively [48]). However, as depicted in Fig. 6, the addition of pyridine and its derivatives had distinctive effects on the conversion of benzyl alcohol. Pyridine remarkably decreased the conversion to 2% in the presence of 1:1 molar ratio of pyridine to benzyl alcohol. Among the other three pyridine derivatives, such effect was not apparent, which was explained by the steric effect arising from methyl, ethyl and di-methyl groups. Such bulky groups were hindered from the pore area, where benzyl alcohol was adsorbed and being activated. If calculating the surface area of the projection of an adsorbed molecule on the adsorbent, the surface area decreased in the sequence: 2, 6-dimethylpyridine (28.1 Å^2) > 2-ethylpyridine (27.7 Å^2) > 2-methylpyridine (22.6 Å^2) > pyridine (17.1 Å^2) [49]. The sequence was in accordance with the decreased conversion of benzyl alcohol. The area of a seven member ring was calculated to be ca. 15 Å^2, which was close to that of pyridine. Among the four additives, only pyridine had the great possibility of adsorbing on the pore area, and the other three molecules were too bulky for the pore area.

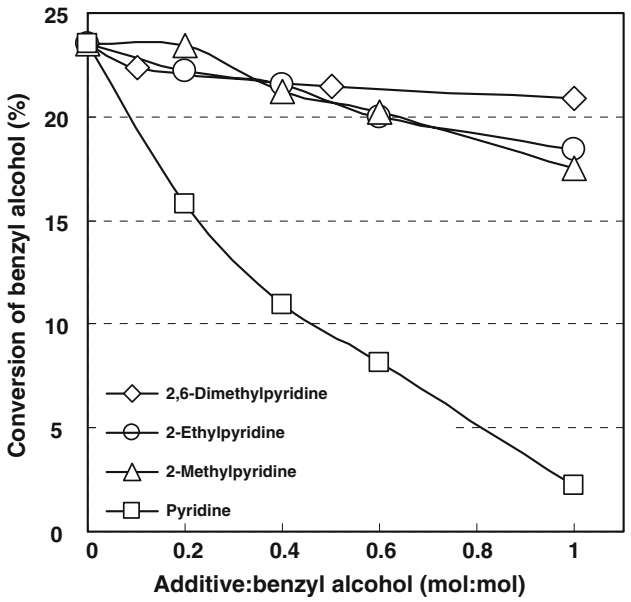

Fig. 6 Effect of pyridine and its derivatives on the catalytic conversion of benzyl alcohol

The competitive adsorption on the pore area between additives and benzyl alcohol might occur. In a typical reaction of using 0.03 g catalyst (S_{BET} 14.7 m^2 g^{-1}), the total catalyst surface area during the reaction was 0.4 m^2. If the additive: benzyl alcohol ratio was 0.1, and 0.07 mmol additive was used, the spread of all additive molecules in a flat surface would occupy 15, 20, 25, and 25 m^2 for pyridine, 2-methylpyridine, 2-ethylpyridine, and 2, 6-dimethylpyridine, respectively, which were 40- to 60-fold of the catalyst area, suggesting that the amount of pyridines are overdose for poisoning all active sites. A competitive adsorption took place because the conversion was not entirely inhibited although excess amount of pyridine was added. A dynamic equilibrium between surface pyridines and solution ones might be established.

The effect of pyridines may simply block the active site, or affect the adsorption of other substances. Coulson and Richardson have used the Eq. 1 to find the ratio of activity of the poisoned catalyst to the activity of the unpoisoned catalyst:

$$F = \frac{\sqrt{1-\sigma}\,\tanh\left(\Phi\sqrt{1-\sigma}\right)}{\tanh\Phi} \quad (1)$$

where F is the ratio of activity of the poisoned catalyst to the activity of the unpoisoned catalyst:

$$\frac{\text{Conversion}_{\text{no addition}} - \text{Conversion}_{\text{addition}}}{\text{Conversion}_{\text{noaddition}}}$$

σ = the fraction of catalyst poisoned
ϕ = Thiele modulus

Pyridine and its derivatives may represent two limiting cases: (a) as pyridine has no steric hindance to active site, the ϕ value is very small, thus F becomes equal to $(1 - \sigma)$ and the loss in activity is linearly connected to the amount of pyridine adsorbed; (b) pyridine derivatives have steric hindrance to reach to active sites, the ϕ value is large, then F becomes $\sqrt{1-\sigma}$ and the activity is less affected than in the presence of pyridine. The plot of the ratio of additive to benzyl alcohol against σ, which was calculated from $(1 - F)$ or $(1 - F^2)$, was depicted in Fig. 7. It can be seen that the dynamic surface fraction covered by pyridine increased to 92%. The other three additives covered <40% when additve: benzyl alcohol ratio was 1:1. Again, the increased coverage of pyridine than the subsituted ones is due to free steric hindrance.

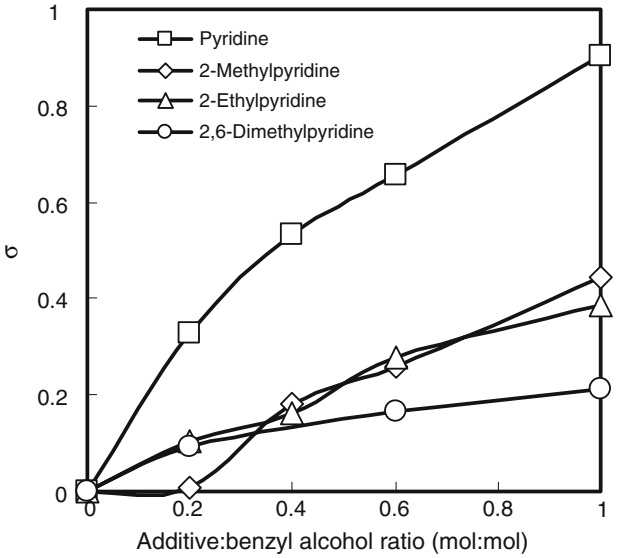

Fig. 7 The fraction (σ) of active sites covered by pyridines with the increasing amount of additives

3.6 The Pyridine Effect of the Selective Oxidation of 1-Hexanol and 2-Hexanol

The effect of pyridine and 2, 6-dimethylpyridine was clearly seen in the oxidation of hexanols as shown in Fig. 8. The addition of 2, 6-dimethylpyridine slightly decreased the conversion of 1-hexanol even 1:1 mole ratio with respect to 1-hexanol was used. The selectivity was 100% to the 1-hexanal. However, 10% of pyridine completely stopped the conversion of 1-hexanol. More interestingly, the addition of 10% pyridine or 2, 6-dimethylpyridine with respect to the amount of 2-hexanol completely stopped the conversion of 2-hexanol. It was believed that the adsorption of 1-hexanol was vertically adsorbed on the pore; the 2-hexanol, due to steric effect, was mainly adsorbed on the non-pore area. Pyridine may compete with 1-hexanol on the acid sites on the pore; and thus the conversion was greatly decreased. However, the 2, 6-dimethylpyridine was sterically hindered to the pore and thus could not compete with 1-hexanol, as a result of which the conversion of 1-hexanol was less affected. Because the 2-hexanol was adsorbed on non-pore area, where both pyridine and 2, 6-dimethylpyridine could be adsorbed, therefore the presence of any additive completely stopped the conversion.

4 Mechanism

The catalytic oxidation of alcohols is believed to take place on the *a*–*b* plane of the Mo–V–O crystal. Because the substrate molecules are too large to enter pore channel completely, the perpendicular adsorption of C–OH group, if there is no bulky group to hinder the interaction, is favorable. The MoO_6 and VO_6 octahedrons along the rim of 6- or 7-member rings expose metal = O sites and also oxygen-defect sites generated during milling and calcining procedure. Such sites remaining approximate distance and space geometry are believed to contribute mostly to the high selectivity of alcohol oxidation.

5 Conclusion

The present study may provide a fundamental understanding of the unique structure of Mo–V–O crystalline oxide in alcohol oxidation under mild conditions. For purpose of control, a non-crystalline Mo–V–O oxide was prepared, and shown to be much less selective to desired products. The substrates of benzyl alcohol, 1-hexanol and cyclohexanol produce aldehydes or ketones as main products. The substrates with methyl groups on the carbon next to alcohol group mainly offer dehydrated products as olefins. The catalytic results with adding substituted pyridines in the oxidation of benzyl alcohol, 1-hexanol and 2-hexanol suggest that the active sites are located around the pore area, and are reachable by pyridine, not by substituted pyridines, such

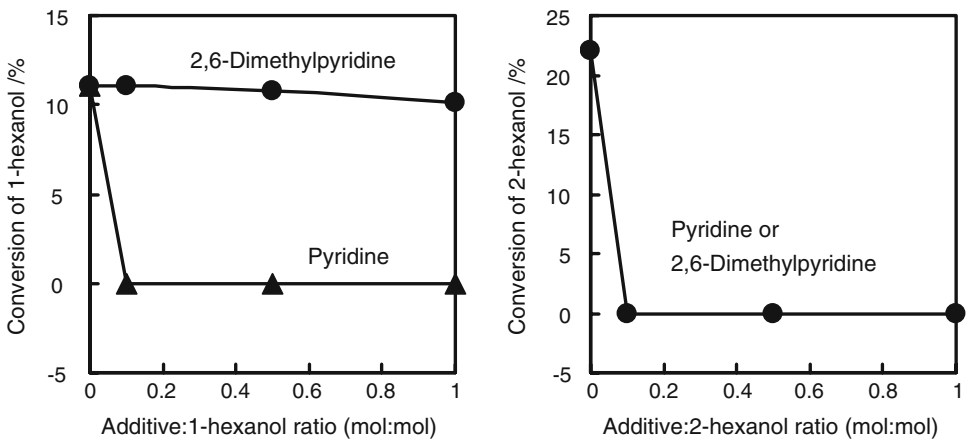

Fig. 8 The effect of pyridine and 2, 6-dimethylpyridine on the conversion of the oxidation of 1-hexanol (*left*) and 2-hexanol (*right*)

as 2-methylpyridine, 2-ethylpyridine and 2, 6-dimethylpyridine. Competitive adsorption on active sites between pyridine and benzyl alcohol remarkably decrease catalytic activity, which 2, 6-dimethylpyridine affects slightly.

Acknowledgement F. Wang would like to acknowledge the financial support of Japan Science and Technology Agency (CREST–JST).

References

1. Cicmanec P, Syslova K, Tichy J (2007) Top Catal 45:229
2. Bhat BR, Choi JS, Kim TH (2007) Catal Lett 117:136
3. Lopez JM (2006) Top Catal 41:3
4. Ivars F, Botella P, Dejoz A, Nieto JML, Concepcion P, Vazquez MI (2006) Top Catal 38:59
5. Bondareva VM, Andrushkevich TV, Aleshina GI, Maksimovskaya RI, Plyasova LM, Dovlitova LS, Burgina EB (2006) React Kinet Catal Lett 88:183
6. Takita Y, Kikutani K, Xia C, Takami H, Nagaoka K (2005) Appl Catal A 283:209
7. Popova GY, Andrushkevich TV, Aleshina GI, Plyasov LM, Khramov MI (2007) Appl Catal A 328:195
8. Giebeler L, Kampe P, Wirth A, Adams AH, Kunert J, Fuess H, Vogel H (2006) J Mol Catal A 259:309
9. Guliants VV, Bhandari R, Swaminathan B, Vasudevan VK, Brongersma HH, Knoester A, Gaffney AM, Han S (2005) J Phys Chem B 109:24046
10. Oliver JM, Nieto JML, Botella P (2004) Catal Today 96:241
11. Safonova OV, Deniau B, Millet JMM (2006) J Phys Chem B 110:23962
12. Grasselli RK, Buttrey DJ, DeSanto P, Burrington JD, Lugmair CG, Volpe AF, Weingand T (2004) Catal Today 91–92:251
13. Grasselli RK, Burrington JD, Buttrey DJ, DeSanto P, Lugmair CG, Volpe AF, Weingand T (2003) Top Catal 23:5
14. Wagner JB, Timpe O, Hamid FA, Trunschke A, Wild U, Su DS, Widi RK, Abd Hamid SB, Schlogl R (2006) Top Catal 38:51
15. Guliants VV, Brongersma HH, Knoester A, Gaffney AM, Han S (2006) Top Catal 38:41
16. Beato P, Blume A, Girgsdies E, Jentoft RE, Schlogel R, Timpe O, Trunschke A, Weinberg G, Basher Q, Hamid FA, Hamid SBA, Omar E, Salim LM (2006) Appl Catal A 307:137
17. Botella P, Garcia-Gonzalez E, Nieto JML, Gonzalez-Calbet JM (2005) Solid State Sci 7:507
18. Schlogl R, Knop-Gericke A, Havecker M, Wild U, Frickel D, Ressler T, Jentoft RE, Wienold J, Mestl G, Blume A, Timpe O, Uchida I (2001) Top Catal 15:219
19. Holmberg J, Hansen S, Grasselli RK, Andersson A (2006) Top Catal 38:17
20. DeSanto P, Buttrey DJ, Grasselli RK, Pyrz WD, Lugmair CG, Volpe AF, Vogt T, Toby BH (2006) Top Catal 38:31
21. Grasselli RK (2005) Catal Today 99:23
22. Grasselli RK, Andersson A, Buttrey DJ, Burrington JD, Lugmair CG, Volpe AF (2004) Abstr Pap Am Chem Soc 228:U490
23. do Santo P, Buttrey DJ, Grasselli RK (2004) Abstr Pap Am Chem Soc 228:U496
24. Buttrey DJ, DeSanto P, Grasselli RK, Vogt T, Toby BH, Volpe AF, Lugmair CG (2004) Abstr Pap Am Chem Soc 227:U1245
25. Holmberg J, Grasselli RK, Andersson A (2004) Appl Catal A 270:121
26. DeSanto P, Buttrey DJ, Grasselli RK, Lugmair CG, Volpe AF, Toby BH, Vogt T (2004) Zeitschrift Fur Kristallographie 219:152
27. Murayama H, Vitry D, Ueda W, Fuchs G, Anne M, Dubois JL (2007) Appl Catal A 318:137
28. Ueda W, Oshihara K (2000) Appl Catal A 200:135
29. Chen NF, Oshihara K, Ueda W (2001) Catal Today 64:121
30. Katou T, Vitry D, Ueda W (2004) Catal Today 91–92:237
31. Ueda W, Vitry D, Katou T (2005) Catal Today 99:43
32. Grasselli RK, Buttrey DJ, Burrington JD, Andersson A, Holmberg J, Ueda W, Kubo J, Lugmair CG, Volpe AF (2006) Top Catal 38:7
33. Ueda W, Endo Y, Watanabe N (2006) Top Catal 38:261
34. Watanabe N, Ueda W (2006) Ind Eng Chem Res 45:607
35. Sadakane M, Watanabe N, Katou T, Nodasaka Y, Ueda W (2007) Angew Chem Int Ed 46:1493
36. Zhan BZ, White MA, Sham TK, Pincock JA, Doucet RJ, Rao KVR, Robertson KN, Cameron TS (2003) J Am Chem Soc 125:2195
37. Yamaguchi K, Mori K, Mizugaki T, Ebitani K, Kaneda K (2000) J Am Chem Soc 122:7144
38. Steinhoff BA, Stahl SS (2006) J Am Chem Soc 128:4348
39. Dijksman A, Marino-Gonzalez A, Payeras AMI, Arends I, Sheldon RA (2001) J Am Chem Soc 123:6826
40. Ishida T, Haruta M (2007) Angew Chem Int Ed 46:7154
41. Sheldon RA, Bekkum Hv (2001) Fine chemicals through heterogeneous catalysis. Wiley-VCH, Weinheim
42. Wang F, Xu J, Li XQ, Gao J, Zhou LP, Ohnishi R (2005) Adv Synth Catal 347:1987
43. Wang F, Ueda W (2008) Chem Lett 37:184
44. Yamashita K, Hirano M, Okumura K, Niwa M (2006) Catal Today 118:385
45. Choudhury J, Podder S, Roy S (2005) J Am Chem Soc 127:6162
46. Nishiguchi T, Machida N, Yamamoto E (1987) Tetrahedron Lett 28:4565
47. Martin JC, Arhart RJ (1971) J Am Chem Soc 93:4327
48. Hunter EPL, Lias SGJ (1998) Phys Chem Ref Data 27 (3):413 and http://webbook.nist.gov
49. Duprat F (1992) Ind Eng Chem Res 31:1907